

Stability of Nitrogen in Planetary Atmospheres in Contact with Liquid Water*

RENYU HU^{1,2} AND HECTOR DELGADO DIAZ¹

¹*Jet Propulsion Laboratory
California Institute of Technology
Pasadena, CA 91109, USA*

²*Division of Geological and Planetary Sciences
California Institute of Technology
Pasadena, CA 91125, USA*

(Received XXX; Revised XXX; Accepted XXX)

Submitted to ApJ

ABSTRACT

Molecular nitrogen is the most commonly assumed background gas that supports habitability on rocky planets. Despite its chemical inertness, nitrogen molecule is broken by lightning, hot volcanic vents, and bolide impacts, and can be converted into soluble nitrogen compounds and then sequestered in the ocean. The very stability of nitrogen, and that of nitrogen-based habitability, is thus called into question. Here we determine the lifetime of molecular nitrogen vis-à-vis aqueous sequestration, by developing a novel model that couples atmospheric photochemistry and oceanic chemistry. We find that HNO, the dominant nitrogen compounds produced in anoxic atmospheres, is converted to N₂O in the ocean, rather than oxidized to nitrites or nitrates as previously assumed. This N₂O is then released back into the atmosphere and quickly converted to N₂. We also find that the deposition rate of NO is severely limited by the kinetics of the aqueous-phase reaction that converts NO to nitrites in the ocean. Putting these insights together, we conclude that the atmosphere must produce nitrogen species at least as oxidized as NO₂ and HNO₂ to enable aqueous sequestration. The lifetime of molecular nitrogen in anoxic atmospheres is determined to be > 1 billion years on temperate planets of both Sun-like and M dwarf stars. This result upholds the validity of molecular nitrogen as a universal background gas on rocky planets.

Keywords: Extrasolar rocky planets — Habitable planets — Super Earths — Exoplanet atmospheric composition — Exoplanet evolution

1. INTRODUCTION

Nitrogen is the bulk constituent of Earth's atmosphere and a common constituent of the atmospheres of rocky planets in the Solar System. The universality of nitrogen has been extended to extrasolar rocky worlds, as molecular nitrogen (N₂) is generally assumed as the background gas in the at-

Corresponding author: Renyu Hu
renyu.hu@jpl.nasa.gov

* ©2019. California Institute of Technology. Government sponsorship acknowledged.

mosphere. The standard picture of habitable planets of stars (Kasting et al. 1993) posits that climate and geologic processes on rocky planets regulate the abundance of atmospheric CO_2 to maintain a surface temperature that is consistent with liquid water oceans – but an often overlooked ingredient of this picture is a constant, approximately 1 bar, N_2 -dominated background atmosphere.

The climate-maintaining effect of N_2 primarily stems from its higher volatility than CO_2 or H_2O . As the partial pressure of CO_2 is controlled by the silicate weathering cycle (Walker et al. 1981), and that of H_2O is controlled by the surface temperature, the partial pressure of N_2 is not a direct function of any climatological parameters. Having a sizable N_2 atmosphere, therefore, alleviates the sensitivity of the planetary climate to subtle changes in forcings, and thus widens the semi-major axis ranges in which the planet can be habitable (Vladilo et al. 2013). No habitable climate can be found if the partial pressure of N_2 is less than 0.015 bar (Vladilo et al. 2013). The actual lower-limit may be even higher, as it is later found that N_2 as a non-condensable gas maintains the cold trap of the middle atmosphere and prevents water from loss to space (Wordsworth & Pierrehumbert 2013). While N_2 is not a greenhouse gas, it causes a warming effect on climate via pressure broadening of CO_2 and H_2O absorption features (Goldblatt et al. 2009).

Due to its strong triple bond, N_2 is very close to being chemically inert in the atmosphere. The processes that can break N_2 are peculiar (Mancinelli & McKay 1988): on today’s Earth it is primarily performed by microbes, and before the rise of nitrogen-fixation microbes it is done in energetic events including lightning (Yung & McElroy 1979; Kasting & Walker 1981; Navarro-González et al. 1998; Wong et al. 2017), bolide impact (McKay et al. 1988), and also hot volcanic vents (Mather et al. 2004). The immediate product of the “atmospheric nitrogen fixation” is NO , and the NO is then converted to HNO_3 in

oxygen-rich atmospheres and to HNO in oxygen-poor ones (Kasting & Walker 1981; Wong et al. 2017). It has been suggested that the HNO is then converted to NO_2^- and NO_3^- in the ocean (Mancinelli & McKay 1988; Summers & Khare 2007). As such, NO produced in the atmosphere eventually becomes nitrites and nitrates. The entire 1-bar N_2 -dominated atmosphere could be sequestered in the ocean as nitrites and nitrates – thus creating a potential problem for the stability of a nitrogen-dominated atmosphere in contact with liquid water oceans.

We are therefore motivated to determine the lifetime of N_2 – and thus that of N_2 -based habitability – on a habitable exoplanet. We focus on anoxic planets without life, because microbes would be able to harvest the nitrites and nitrates in the oceans, reduce them to N_2 or N_2O , and restore the N_2 stability. Without life, the formation of nitrites and nitrates may well be mostly one-way and become long-term losses of nitrogen. In this paper we calculate the kinetic timescale of this process. We first study the fate of HNO , the dominant nitrogen compound produced in anoxic atmospheres, when it is deposited into the ocean. We show that HNO does not lead to nitrogen sequestration but rather formation of N_2O (Section 2). We then present a novel model that couples an atmosphere photochemistry model (Hu et al. 2012; Hu et al. 2013) and an ocean aqueous-chemistry model, so that the rates of transfer between the atmosphere and the ocean can be self-consistently calculated (Section 3). Using the coupled model we determine the lifetime of N_2 in anoxic atmospheres on temperate planets of Sun-like and M dwarf stars (Section 4). We discuss the implications of our findings in Section 5 and conclude in Section 6.

2. AQUEOUS CHEMISTRY OF HNO ON PLANETS

2.1. *Aqueous-Phase Reactions and Kinetic Rates*

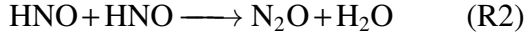
HNO is the main atmospheric product of nitrogen compounds under anoxic conditions, and its

fate in the ocean has not been clarified. The aqueous chemistry of HNO, and its conjugate base NO^- , is peculiar because the ground state of HNO is a singlet while that of NO^- is a triplet. This makes the deprotonation reaction to proceed as the forward direction of



a slow, second-order reaction (Miranda 2005). Under the pH conditions relevant to planets, most of the dissolved HNO exists in the form of HNO. We note that the excited state HNO is a triplet and it quickly dissociates to NO^- . The transition to the excited state, however, is spin forbidden and has not been observed in experiments.

Dissolved HNO can be removed by rapid dehydrative dimerization

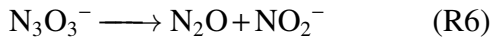


with its rate constant determined by the flash photolysis technique (Shafirovich & Lyman 2002).

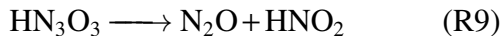
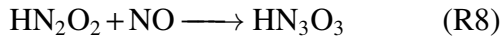
NO^- is rapidly oxidized to nitrate when free oxygen is available



or polymerized by NO via



The polymerization can also start from HNO



Both polymerization reactions eventually form N_2O and nitrite, and their rate constants have been measured using pulse radiolysis and NO-rich fluids (Gratzel et al. 1970; Seddon et al. 1973). These polymerization pathways have been adopted as the pathway to convert HNO to nitrite and nitrate in planetary oceans (Mancinelli & McKay 1988; Summers & Khare 2007; Wong et al. 2017).

In summary, the removal pathways of HNO in the aqueous phase are dehydrative dimerization (Reaction R2), deprotonation (Reaction R1) followed by either oxidation (Reaction R3) or polymerization (Reactions R4-R6), and direct polymerization (Reactions R7-R9). Relevant rate constants are tabulated in Table 1.

Reaction	Rate Constant
R1 forward	$5 \times 10^4 \text{ M}^{-1} \text{ s}^{-1}$
R1 reverse	$1.2 \times 10^2 \text{ s}^{-1}$
R2	$8 \times 10^6 \text{ M}^{-1} \text{ s}^{-1}$
R3	$4 \times 10^9 \text{ M}^{-1} \text{ s}^{-1}$
R4 forward	$2 \times 10^9 \text{ M}^{-1} \text{ s}^{-1}$
R4 reverse	$3 \times 10^4 \text{ s}^{-1}$
R5	$3 \times 10^6 \text{ M}^{-1} \text{ s}^{-1}$
R7 forward	$2 \times 10^9 \text{ M}^{-1} \text{ s}^{-1}$
R7 reverse	$8 \times 10^6 \text{ s}^{-1}$
R8	$8 \times 10^6 \text{ M}^{-1} \text{ s}^{-1}$
R10	$2 \times 10^8 \text{ M}^{-1} \text{ s}^{-1}$
R11	$1 \times 10^8 \text{ M}^{-1} \text{ s}^{-1}$

Table 1. Rate constants for HNO, NO, and NO_2 reactions in the aqueous phase. Compiled from Miranda (2005) and Lee (1984). The rate constants are provided at the room temperature.

2.2. Reaction Rates under Planetary Conditions

Using the kinetic constants from experiments, we calculate the reaction rates of the HNO removal pathways under typical planetary conditions.

After deprotonation, NO^- can be either oxidized (Reaction R3) or polymerized (Reactions R4-R6). We first compare the two sub-pathways. The rate

of Reaction (R3) is

$$R_{R3} = k_{R3}[\text{NO}^-][\text{O}_2], \quad (1)$$

and the overall rate of Reactions (R4-R6) is

$$R_{R4-R6} = k_{R4_f}[\text{NO}^-][\text{NO}] \frac{k_{R5}[\text{NO}]}{k_{R4_r} + k_{R5}[\text{NO}]}, \quad (2)$$

where the additional f and r in the subscript denote the rate constant of the forward and the reverse directions, respectively, and quantities in $[X]$ denote the concentration of the species X in the aqueous phase, usually in the unit of M (i.e., mole per liter). The reaction rate R has the unit of M s^{-1} .

Species	Typical	Upper Limit
f_{NO}	4×10^{-11}	3×10^{-6}
$[\text{NO}]$	$8 \times 10^{-14} \text{ M}$	$6 \times 10^{-9} \text{ M}$
f_{O_2}	2×10^{-15}	1×10^{-8}
$[\text{O}_2]$	$2 \times 10^{-18} \text{ M}$	$1 \times 10^{-11} \text{ M}$
f_{HNO}	2×10^{-11}	2×10^{-10}
$[\text{HNO}]$	$2 \times 10^{-10} \text{ M}$	$2 \times 10^{-9} \text{ M}$

Table 2. Typical and anoxic upper-limit concentrations for evaluating and comparing the reaction rates of HNO removal pathways. For each gas (X), the mixing ratio at the bottom of the atmosphere (f_X) and the concentration in the surface ocean ($[X]$) are provided. These quantities are consistent with the converged photochemistry models shown in Section 4.

For a typical anoxic condition, $[\text{NO}] \sim 8 \times 10^{-14} \text{ M}$ and $[\text{O}_2] \sim 2 \times 10^{-18} \text{ M}$ (Table 2). These quantities are from the atmospheric photochemistry models under terrestrial lightning rates (Section 4) and have factored in the Henry's law constants for respective gases. When the lightning rate is very high (i.e., $100\times$ the terrestrial rate), the upper limits are $[\text{NO}] \sim 6 \times 10^{-9} \text{ M}$ and $[\text{O}_2] \sim 10^{-11} \text{ M}$. Note that these upper limits do not include the oxygen-rich scenarios that would be produced on planets of M dwarf stars (see Section 4).

Based on these concentrations, $R_{R4-R6} = 10^{-15} \sim 10^{-10}[\text{NO}^-] \text{ M s}^{-1}$ and $R_{R3} = 10^{-8} \sim 4 \times 10^{-2}[\text{NO}^-]$

M s^{-1} . Therefore, even under the anoxic conditions, $R_{R3} \gg R_{R4-R6}$, and the same is true for oxygen-rich conditions. The overall rate of the removal path starting with deprotonation (Reaction R1) is thus

$$R_{R1} = k_{R1_f}[\text{HNO}][\text{OH}^-] \frac{k_{R3}[\text{O}_2]}{k_{R1_r} + k_{R3}[\text{O}_2]}. \quad (3)$$

The rate of dehydrative dimerization (Reaction R2) is

$$R_{R2} = k_{R2}[\text{HNO}][\text{HNO}], \quad (4)$$

and the overall rate of direct polymerization (Reactions R7-R9) is

$$R_{R7-R9} = k_{R7_f}[\text{HNO}][\text{NO}] \frac{k_{R8}[\text{NO}]}{k_{R7_r} + k_{R8}[\text{NO}]}. \quad (5)$$

Under typical and limiting anoxic conditions, $[\text{HNO}] \sim 2 \times 10^{-10} - 2 \times 10^{-9} \text{ M}$ (Section 4). For a neutral pH, we estimate $R_{R1} = 7 \times 10^{-23} \sim 3 \times 10^{-15} \text{ M s}^{-1}$, $R_{R2} = 3 \times 10^{-13} \sim 3 \times 10^{-11} \text{ M s}^{-1}$, and $R_{R7-R9} = 3 \times 10^{-27} \sim 10^{-16} \text{ M s}^{-1}$. Comparing the three rates, we have $R_{R2} \gg R_{R1} > R_{R7-R9}$. R_{R1} is proportional to the concentration of OH^- in the ocean, and for R_{R1} to be greater than R_{R2} , the ocean must be highly alkaline with $\text{pH} > 11$. Such a pH value is well higher than the pH of Earth's ocean currently or in the Archean (Halevy & Bachan 2017; Krissansen-Totton et al. 2018). Therefore, under anoxic conditions relevant for planetary atmospheres, dehydrative dimerization (Reaction R2) is the dominant removal pathway of HNO deposited in the ocean.

Under oxygen-rich conditions, including in the oxygen-rich atmospheres produced by CO_2 photolysis on planets of M dwarf stars (see Section 4), little HNO is produced in the atmosphere, and thus the dissolved concentration is very small. In this case, the rate of Reaction (R2) is very small, and deprotonation followed by oxidation (Reactions R1 and R3) dominates. However, that HNO oxidation pathway is still not important to the overall removal flux of nitrogen, because little HNO is produced in the atmosphere in the first place.

2.3. Consistency with *Summers & Khare (2007)*

The main finding of this section is that under planetary conditions the deposited HNO in the ocean does not mainly become nitrite or nitrate. This finding might be perceived as contradictory to the experimental result of *Summers & Khare (2007)*, where a gas mixture of CO₂ and N₂ with 1% NO and 1% CO in contact with liquid water was irradiated by ultraviolet light. *Summers & Khare (2007)* found that nitrate and nitrite to a lesser extent were formed and the NO was depleted in approximately 1 hour. A smaller amount of N₂O was also produced. The interpretation was that HNO was formed and dissolved, and Reactions (R4-R6) or Reactions (R7-R9) took place dominantly in the system.

The experimental result of *Summers & Khare (2007)* is consistent with our model of the kinetics of HNO aqueous chemistry, as it showcases the outcome from a NO-rich fluid. The experimental vessel was filled to a pressure of approximately 1 bar, which means that in equilibrium $[\text{NO}] \sim 2 \times 10^{-5}$ M. Therefore, the fluid was more NO-rich than planetary oceans by orders of magnitude. Applying this concentration and re-evaluating all reaction rates in this section, we find that the rate of Reaction (R1) followed by Reactions (R4-R6) is $2 \times 10^{-3}[\text{HNO}] \text{ M s}^{-1}$, the rate of Reactions (R7-R9) is $8 \times 10^{-1}[\text{HNO}] \text{ M s}^{-1}$, and the rate of Reaction (R2) is $8 \times 10^6[\text{HNO}]^2 \text{ M s}^{-1}$. The concentration of HNO in the system is unknown, but NO has a lifetime of 1 hour and yet [HNO] has a lifetime of at most ~ 1 s. As an upper limit, we assume that HNO is the only intermediary in the removal of NO and that all HNO in the system (a 110-ml gas cell) is in the aqueous phase (15-ml water, *Summers & Khare (2007)*). We estimate $[\text{HNO}] < 7 \times 10^{-7}$ M. Together, we find that even at this upper limit, the reaction rate of direct polymerization (Reactions R7-R9) is on the same order of magnitude as the reaction rate of dehydrative dimerization (Reaction R2). In reality, the concentration of HNO should

be smaller and polymerization becomes the dominant pathway, with the N₂O-producing dimerization the secondary pathway. This is what was seen in the experiment, and our kinetic model is thus consistent with the experiment.

2.4. *The Fate of HNO in Planetary Oceans*

To summarize, the analysis in this section shows that under planetary conditions most of the deposited HNO undergoes dehydrative dimerization, and becomes N₂O. The dehydrative dimerization is kinetically favored over oxidization to nitrate or polymerization to nitrite by at least four orders of magnitude under anoxic conditions, and in most cases, by ten orders of magnitude.

The insight we obtain here by evaluating the kinetic rates of HNO removal pathways clarifies the fate of HNO produced in anoxic atmospheres and deposited in the oceans. Models of the atmospheric evolution for Earth and planets have assumed that the HNO would quickly become nitrite and nitrate in the ocean (*Mancinelli & McKay 1988; Wong et al. 2017; Laneuville et al. 2018; Ranjan et al. 2019*). The experimental basis for this early assumption was the pulse radiolysis experiments for Reactions R4-R6 and R7-R9 (*Gratzel et al. 1970; Seddon et al. 1973*) and the experiment of *Summers & Khare (2007)*. These experiments used NO-rich fluids, and thus to apply their results one must evaluate the implied kinetic rates for reasonable planetary conditions and compare with other potential reaction pathways. Here we show that for anoxic atmospheres, dehydrative dimerization is the dominant pathway, and for oxygen-rich atmospheres, deprotonation followed by oxidation is the dominant pathway. These results are also testable by experiments in the laboratory.

It is therefore reasonable to consider Reaction (R2) the sole reaction of HNO in the aqueous phase. The produced N₂O, because of its low solubility, is released to the atmosphere and eventually photolyzed to become N₂. The formation of HNO in the atmosphere is thus not an effective path to-

ward nitrite or nitrate, and does not lead to sequestration of molecular nitrogen in the aqueous phase.

3. COUPLED ATMOSPHERE-OCEAN MODEL

We develop an ocean chemistry module and couple it with the atmospheric photochemistry model of [Hu et al. \(2012\)](#); [Hu et al. \(2013\)](#) to determine the lifetime of N_2 in anoxic atmospheres in contact with liquid-water oceans. The photochemistry model has been validated by computing the atmospheric compositions of present-day Earth and Mars, as the outputs agreed with the observations of major trace gases in Earth’s and Mars’ atmospheres ([Hu 2013](#)). The model includes a comprehensive reaction network for O, H, C, N, and S species including sulfur and sulfuric acid aerosols, and its applications to simulating anoxic atmospheres and maintaining the redox flux balance of the atmosphere and the ocean have been well-documented ([James & Hu 2018](#)) and compare well with other photochemical models ([Gao et al. 2015](#); [Harman et al. 2018](#)).

For this work, we choose to simulate a 1-bar atmosphere of 95% N_2 and 5% CO_2 , as this kind of anoxic atmosphere is akin to the O_2 -poor and CO_2 -rich environment of the Archean Earth, and is often adopted as the archetype for anoxic exoplanet atmospheres (e.g., [Tian et al. 2014](#); [Domagal-Goldman et al. 2014](#); [Harman et al. 2015](#)). We assume a surface temperature of 288 K and a stratospheric temperature of 200 K and include volcanic outgassing of CO, H_2 , SO_2 , and H_2S in the same way as in [James & Hu \(2018\)](#). We use the entire reaction network of the atmospheric photochemistry model of [Hu et al. \(2012\)](#); [Hu et al. \(2013\)](#), except the organic compounds that have more than two carbon atoms and their reactions. The outgassing rate adopted here is not high enough to produce a H_2SO_4 aerosol layer in the atmosphere.

We include both a Sun-like star and an M dwarf star as the parent star. For the M dwarf star, we use GJ 876 as the representing case and apply its

measured spectrum in the ultraviolet ([France et al. 2016](#)) in the photochemistry model.

To simulate the effect of atmospheric nitrogen fixation, we start from the terrestrial production rate of NO by lightning, $6 \times 10^8 \text{ cm}^{-2} \text{ s}^{-1}$ ([Schumann & Huntrieser 2007](#)). Changing the main oxygen donor from O_2 to CO_2 and H_2O would lead to approximately one-order-of-magnitude less NO, but the lightning rate also depends on how convective the atmosphere is ([Wong et al. 2017](#); [Harman et al. 2018](#)). Besides, bolide impacts and hot volcanic vents may also contribute substantially to the source of NO ([McKay et al. 1988](#); [Mather et al. 2004](#)). We therefore explore the effect of changing NO flux by three orders of magnitude from the terrestrial lightning value to cover these varied scenarios. Also, assuming the oxygen comes from CO_2 , each molecule of NO produced is accompanied by another molecule of CO. We include this conjugate CO source in the model, and in this way, no net redox change is introduced to the atmosphere.

3.1. Ocean Chemistry and Deposition Velocities of Nitrogen Species

Chemical reactions in the ocean affect the atmospheric photochemistry model by adjusting the rate of gas exchange between the atmosphere and the ocean. Conceptually, the transfer flux from the atmosphere to the ocean can be expressed as $\phi = v_{\max}(n - MC/H) = v_{\text{dep}}n$ where v_{\max} is the maximum deposition velocity and v_{dep} is the effective deposition velocity, n is the number density at the bottom of the atmosphere, M is the concentration at the surface ocean, H is Henry’s law constant, and C is a unit conversion factor depending on the definition of Henry’s law constant ([Kharecha et al. 2005](#)). The effective deposition velocity depends on how fast the ocean can “process” the deposited gas: if the ocean removes the gas quickly, then $M \rightarrow 0$, and $v_{\text{dep}} \rightarrow v_{\max}$; whereas if the ocean cannot remove the gas, Henry’s law equilibrium could be established, and in this case, $M \rightarrow nH/C$ and $v_{\text{dep}} \rightarrow 0$. v_{\max} can be approxi-

mated by the speed for the gas to diffuse through laminar layers at the interface between the atmosphere and the ocean, aka. the two-film model (Broecker & Peng 1982) and is sensitive to the solubility of the gas, the wind speed, and the temperature (Domagal-Goldman et al. 2014; Harman et al. 2015). For highly soluble species $v_{\max} \sim 1 \text{ cm s}^{-1}$ and for weakly soluble ones, $v_{\max} \sim 10^{-4} - 10^{-3} \text{ cm s}^{-1}$.

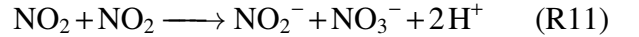
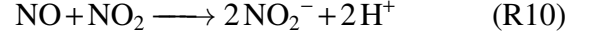
Species	Deposition velocity cm s^{-1}
N_2O	0
NO	calculated iteratively
NO_2	calculated iteratively
NO_3	1
N_2O_5	1
HNO	calculated iteratively
HNO_2	1
HNO_3	1
HNO_4	1

Table 3. Effective deposition velocities for nitrogen species.

Table 3 lists the effective deposition velocities for nitrogen species. We do not include any process that removes N_2O in the ocean, and thus its deposition velocity is zero. For HNO_2 and HNO_3 , the ocean’s capacity to store them is vast, and thus we assume that they are permanently lost to the ocean once deposited, and their deposition velocities approach v_{\max} . NO_3 , N_2O_5 , and HNO_4 quickly react or decomposes to NO_3^- , and thus they are also considered permanently lost once deposited. Over geologic timescales the dissolved NO_2^- and NO_3^- can be reduced to NH_4^+ , or to NO, N_2O , and N_2 and released back to the atmosphere, by cycling through hydrothermal vents (Wong et al. 2017; Laneuville et al. 2018), and ultraviolet photolysis and reduction by Fe^{2+} (e.g., Stanton et al. 2018; Ranjan et al. 2019). This potential source of gaseous NO and N_2O is not included in the current model since we explore a wide range of NO flux

as the boundary condition, and the N_2O is readily photodissociated in the atmosphere.

For NO, NO_2 , and HNO, we solve for their concentrations in the ocean, using the rates of Reaction (R2) and the following reactions in the aqueous phase:



The rate constants of Reactions (R10) and (R11) are from Lee (1984) and tabulated in Table 1. For each mixing ratio (or partial pressure) of NO, NO_2 , and HNO at the bottom of the atmosphere, their steady-state concentrations in the ocean can be calculated, assuming homogeneous distribution in the ocean. The results are then expressed in the effective deposition velocities and are shown in Figure 1.

Several important observations can be drawn from Figure 1. (1) NO does not substantially transfer to the ocean unless the mixing ratio of NO_2 is approaching 1 ppm. This is because the removal of NO by Reaction (R10) requires another NO_2 . The conditions for such a large abundance of NO_2 at the surface is rarely achieved. The effective deposition velocity of NO can be large when the mixing ratio of NO is very small. This however does not imply a substantial transfer flux because the flux is the product of the deposition velocity and the mixing ratio. The deposition flux of NO is thus severely limited by the kinetic rate of Reaction (R10). (2) NO_2 practically deposits at v_{\max} . Unless the lightning rate is very small, the partial pressure of NO is always high enough to effectively remove NO_2 via Reaction (R10). Even when the mixing ratio of NO is indeed very small (see Figure 1, middle panel, yellow line), Reaction (R11) can efficiently remove the dissolved NO_2 and make the deposition velocity to approach v_{\max} for a mixing ratio of NO_2 greater than 10^{-12} . Since the deposition flux would always be small at the low end of the lightning

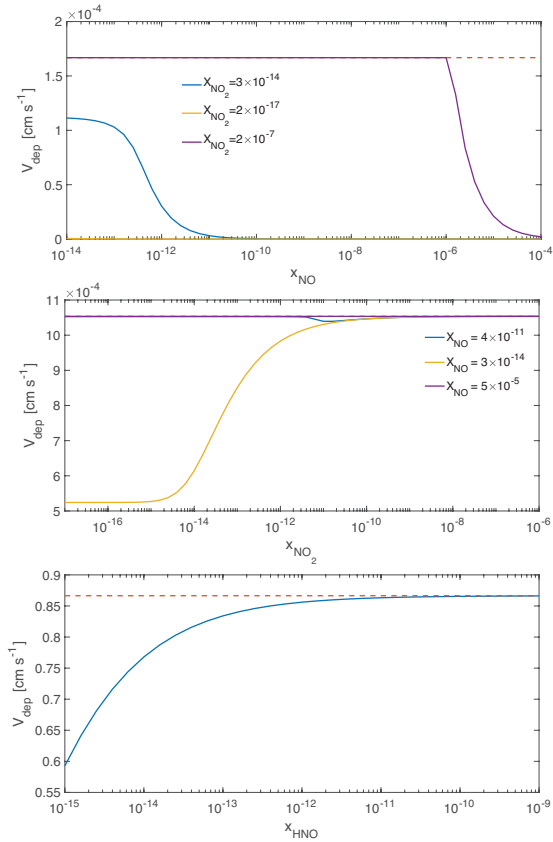


Figure 1. Effective deposition velocities of NO, NO₂, and HNO as a function of the partial pressure at the bottom of the atmosphere. The dashed lines show v_{\max} . The deposition velocities of NO and NO₂ depend on the partial pressure of the other gas. For this reason, three cases are shown, with typical (blue lines), low (yellow lines), and high (purple lines) abundances of the other gas. The calculations are performed for a 3-km deep, homogeneous ocean.

rate, Figure 1 indicates that in practice the deposition of NO₂ is always efficient. (3) The deposition of HNO is generally quite efficient, with v_{dep} close to v_{\max} . But as shown in Section 2, this deposition leads to a return flux of N₂O to the atmosphere.

Because the effective deposition velocities depend on the partial pressure at the bottom of the atmosphere, we need to solve the coupled atmosphere-ocean chemistry model iteratively. For each scenario, we typically start with v_{\max} . Once a steady-state solution is found for the atmospheric chemistry, we use the mixing ratio of NO, NO₂, and HNO at the bottom of the atmosphere to cal-

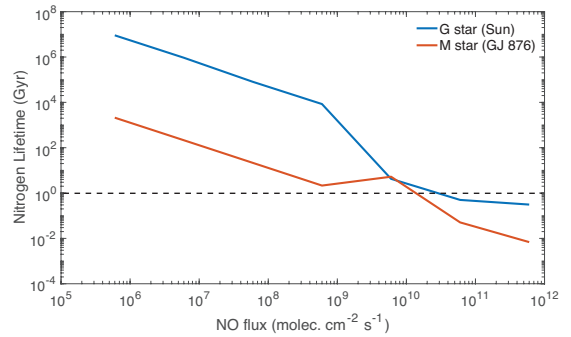


Figure 2. Lifetime of molecular nitrogen in planetary atmospheres in contact with liquid water oceans. The dashed line shows 1 billion years for comparison. Lightning in Earth’s atmosphere produces a NO flux of 6×10^8 molecule $\text{cm}^{-2} \text{s}^{-1}$. The lifetime is well greater than 1 billion years unless the NO source flux is particularly strong.

culate their effective deposition velocities. We also add the corresponding return flux of N₂O as part of the revised boundary conditions. We then relaunch the atmospheric chemistry calculation and find a new steady-state solution. This procedure is repeated until the steady-state mixing ratios of NO, NO₂, and HNO no longer change. Typically only a handful of iterations are required. As such, we can find self-consistent solutions that satisfy both the atmosphere and ocean chemistry.

To summarize, the analysis presented so far indicates that the deposition of NO or HNO cannot be a net sink for molecular nitrogen in the atmosphere, because NO does not deposit efficiently and HNO deposition leads to a return flux of N₂O. Therefore, to sequester nitrogen in the ocean, the atmosphere must oxidize nitrogen compounds to at least as oxidized as NO₂ and HNO₂. With this insight, we will show in Section 4 that this required oxidation is quite slow in anoxic atmospheres and molecular nitrogen is therefore kinetically stable.

4. RESULTS

The lifetime of molecular nitrogen in planetary atmospheres in contact with a liquid-water ocean for varied NO fluxes from lightning and other energetic processes is shown in Figure 2. The lifetime is calculated from the deposition fluxes of

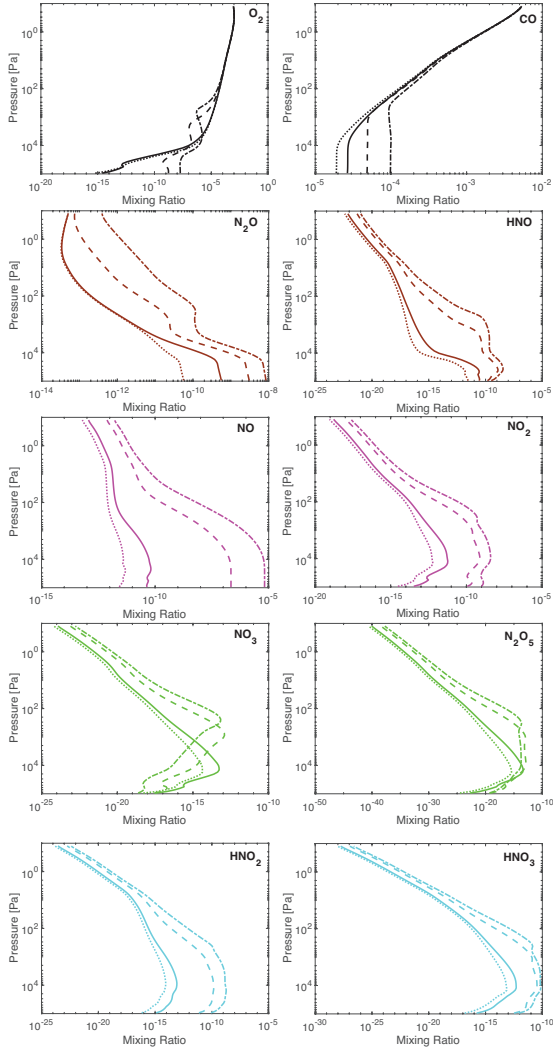


Figure 3. The atmospheric abundances of O_2 , CO , and main nitrogen species in an N_2 -dominated atmosphere on a temperate rocky planet of a Sun-like star. Note that the horizontal axis of each panel is different. Dotted, solid, dashed, and dash-dot lines are from converged atmosphere-ocean chemistry models with an NO flux of 6×10^7 , 6×10^8 (terrestrial value), 6×10^9 , 6×10^{10} molecule $\text{cm}^{-2} \text{s}^{-1}$, respectively. The source strength of NO has a variety of impact and feedback on the nitrogen chemistry in the atmosphere (see text).

NO , NO_2 , NO_3 , N_2O_5 , HNO_2 , HNO_3 , and HNO_4 , from the converged atmosphere-ocean chemistry solutions. The atmospheric abundances of these species are shown in Figures 3 and 4. The deposition flux of HNO is not included in the calculation of the lifetime, as it is returned to the atmosphere in the form of N_2O (Section 2). With the effective

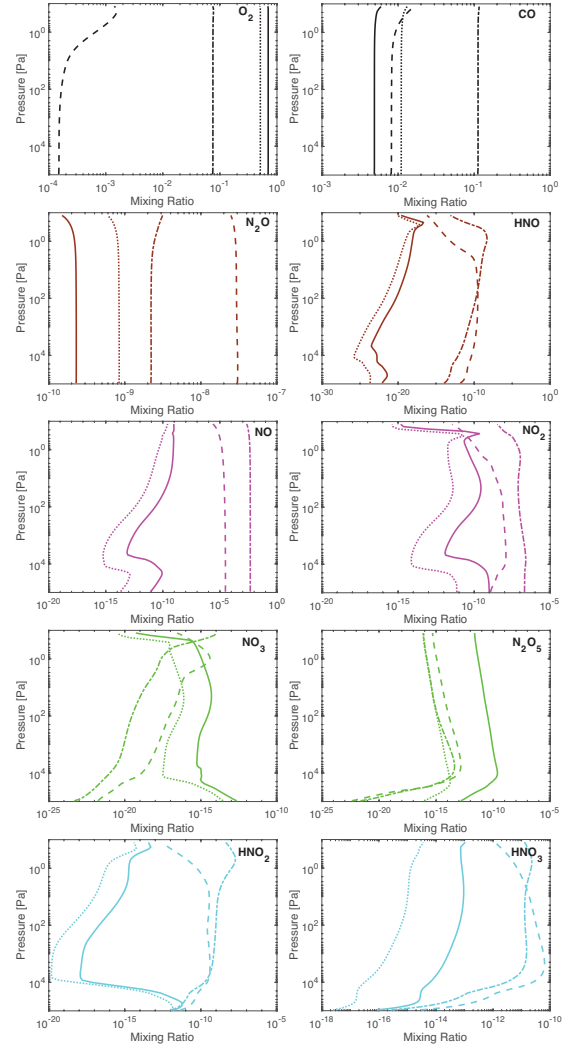


Figure 4. The same as Figure 3 but with GJ 876 as the parent star. The atmosphere becomes O_2 -rich at the steady state due to CO_2 photolysis, and this effect has a strong impact on the nitrogen chemistry (see text).

deposition velocities calculated self-consistently from the ocean-chemistry models (Figure 5), the deposition fluxes of weakly soluble species (NO and NO_2) represent how fast the ocean can process them.

The lifetime of molecular nitrogen is well longer than 1 billion years unless the NO flux is > 100 times larger than the present-day Earth's lightning production rate. Interestingly, we see that the lifetime of nitrogen on planets around Sun-like stars is longer than that on planets around M dwarf stars. For instance, the lifetime under the lightning rate

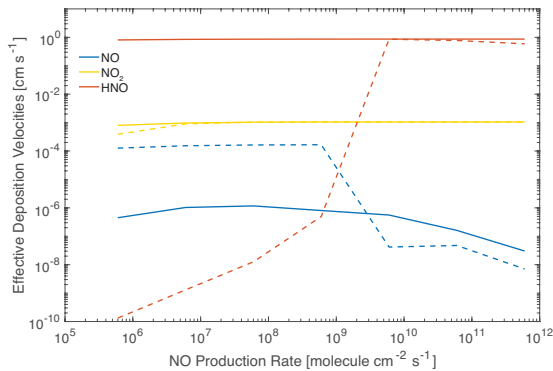


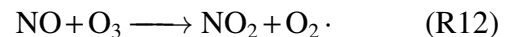
Figure 5. Effective deposition velocities in the converged atmosphere-ocean chemistry solutions. Solid lines are from the Sun-like star cases, and dashed lines are from the GJ 876 cases. The effective deposition velocities are self-consistently calculated, and are different from case to case.

of present-day Earth is ~ 2 billion years on an M dwarf’s habitable planet, and that on a Sun-like star’s habitable planet is 4-order-of-magnitude longer.

The atmospheric nitrogen chemistry is substantially modified with the inclusion of the oceanic feedback, i.e., the inability to deposit NO and the return flux of N_2O . For a Sun-like star as the parent star, the atmosphere is always poor in O_2 (Figure 3), and thus oxidizing NO is difficult. For a higher NO production rate, the steady-state mixing ratios of NO, NO_2 , and HNO increase, and so is the return flux of N_2O . The steady-state mixing ratio of N_2O thus also increases. The upper limit of the N_2O mixing ratio obtained from our model is $\sim 10^{-8}$, still much smaller than that in present-day Earth’s atmosphere ($\sim 3 \times 10^{-7}$). The dominant form of nitrogen deposition is HNO_3 when the NO flux is $\leq 6 \times 10^8$ molecule $cm^{-2} s^{-1}$, and it becomes HNO_2 when the NO flux is $\geq 6 \times 10^9$ molecule $cm^{-2} s^{-1}$. The surface abundance and thus the deposition rate of HNO is larger than HNO_2 and HNO_3 – it is however not counted as a net loss of atmospheric nitrogen. The steady-state mixing ratio of NO can accumulate to a quite high level, and this is made possible by its very small effective deposition velocity (Figure 5). In other words, the ocean cannot process the NO so quickly. For the

same reason, even a large surface abundance NO does not imply a major deposition pathway.

The situation is more complex when the parent star is an M dwarf. Because M dwarfs emit strongly in the far-ultraviolet bandpass but weakly in the near-ultraviolet bandpass, their rocky planets in the habitable zone tend to accumulate O_2 from photolysis of CO_2 (Tian et al. 2014; Domagal-Goldman et al. 2014; Harman et al. 2015). The NO- NO_2 catalytic cycle initiated by lightning cannot remove the photochemical O_2 on an M dwarf’s planet either (Hu et al. 2019, ApJ, submitted). Here we find the same phenomenon of abiotic O_2 accumulation, and the exact amount of O_2 has to do with the assumed NO flux from lightning (Harman et al. 2018, and Hu et al. 2019, ApJ, submitted). The accumulation of abiotic O_2 is not the focus of this paper, but the availability of free oxygen does impact the nitrogen chemistry and greatly reduces the lifetime of N_2 . With the free oxygen, the atmosphere has up to 10 ppm of O_3 in the stratosphere and is thus able to efficiently oxidize NO via



Compared to the Sun-like star cases, the M star cases have higher abundances of NO_2 , NO_3 , and HNO_2 at the steady state. The higher abundance of NO_2 also helps deposition of NO via Reaction (R10). HNO is practically not produced in the atmosphere unless the NO flux from lightning is $\geq 6 \times 10^9$ molecule $cm^{-2} s^{-1}$. When it is produced, the corresponding return flux of N_2O can drive the atmospheric N_2O to up to 3×10^{-8} . To compare, the terrestrial (biological) emission rate of N_2O would lead to a much higher abundance of $\sim 10^{-6}$ (Segura et al. 2005). The response of HNO and N_2O to an increasing lightning rate is not monotonic, and this reflects the competing effects of free oxygen, and a low level of near-ultraviolet irradiation and low abundances of OH and HO_2 in the atmosphere.

5. DISCUSSION

5.1. *Lifetime of Nitrogen on Archean Earth*

We can apply the results to Archean Earth as the modeled atmosphere irradiated by a Sun-like star has an oxidation state similar to Earth before the rise of oxygen. Except for bolide impact that concentrated in the earliest time (McKay et al. 1988), the production rate of NO from lightning and hot volcanic vents would be in the range of $6 \times 10^7 \sim 6 \times 10^8$ molecule $\text{cm}^{-2} \text{s}^{-1}$ (Mather et al. 2004; Wong et al. 2017; Harman et al. 2018). With this input, we find that the total flux of nitrogen deposition would in the range of $1.6 \times 10^4 \sim 1.5 \times 10^5$ molecule $\text{cm}^{-2} \text{s}^{-1}$. In other words, only $\sim 0.03\%$ of the reactive nitrogen produced in the atmosphere is permanently lost to the ocean. The lifetime of nitrogen is 10^4 billion years or larger, implying that the N_2 atmosphere is stable without any help from nitrate-consuming microbes.

Of the deposition flux of nitrogen species, approximately 80% is HNO_3 and 20% is HNO_2 . The flux of nitrate deposition we calculate is consistent in the ballpark with Wong et al. (2017) but we clarify the oceanic feedback to the gas deposition and we remove HNO from effective deposition. Assuming that the residence time of this nitrite and nitrate is determined by the ocean cycling through high-temperature hydrothermal vents (~ 0.4 billion years, Wong et al. 2017), and an average ocean depth of ~ 3 km, we estimate the concentration of nitrate to be $0.9 - 9 \mu\text{M}$, and that of nitrite to be $0.2 - 2 \mu\text{M}$ in the Archean ocean. If circulation through all hydrothermal vents causes the removal of nitrite and nitrate (Laneuville et al. 2018), the residence time reduces to ~ 10 million years and the nitrate and nitrite concentrations further reduce by two orders of magnitude.

Cycling through hydrothermal vents is probably not the only way to remove nitrite and nitrate in the ocean. Ranjan et al. (2019) compares the kinetic loss rate of oceanic nitrite and nitrate due to hydrothermal vents, ultraviolet photolysis (Zafiriou 1974; Carpenter & Nightingale 2015), and reactions with reduced iron (Jones et al.

2015; Buchwald et al. 2016; Grabb et al. 2017; Stanton et al. 2018). The loss rates due to photolysis and reactions with reduced iron can be greater than that due to hydrothermal vents by orders of magnitude. This implies that the concentrations of nitrite and nitrate we estimate in this section is an upper limit and the actual concentrations can be much lower.

5.2. *Abiotic N_2O in Anoxic Atmospheres*

In this work we show that HNO produced in the atmosphere would become N_2O when an aqueous environment exists. One might ask if this source of N_2O constitutes a “false positive” for using N_2O as a biosignature gas (e.g., Des Marais et al. 2002). With the coupled atmosphere-ocean model, we find that the abundance of N_2O produced by HNO dehydrative dimerization is always smaller than the abundance of N_2O that would be produced from a source strength of current Earth’s biosphere, by more than one order of magnitude, but it can be comparable to a lower biological N_2O production in Earth’s anoxic past (e.g. Rugheimer & Kaltenecker 2018). This is true for either a Sun-like star or an M star as the parent star. The difference in the N_2O mixing ratio by more than one order of magnitude causes an appreciable difference in the N_2O spectral features in the infrared (e.g. Rugheimer & Kaltenecker 2018). The use of N_2O as a biosignature gas thus requires the detection of its source strength at the level of current Earth’s biosphere.

6. CONCLUSION

We present a coupled atmosphere-ocean chemistry model to study the lifetime of molecular nitrogen (N_2) in planetary atmospheres in contact with a liquid-water ocean. The question of lifetime exists because nitrogen is the background gas for canonical planetary habitability scenarios and because nitrogen could be sequestered in the ocean when it is chemically converted to soluble compounds like nitrites and nitrates.

We clarify several important features of nitrogen's aqueous-phase chemistry for planetary applications. First, we find that dehydrative dimerization is the main loss pathway of HNO, the dominant nitrogen species produced in anoxic atmospheres. This reaction produces N₂O, which is then released to the atmosphere and photodissociated to become N₂. This finding corrects the long-standing assumption that the HNO would eventually become nitrate in the ocean. Second, we find that the deposition flux of NO is always very small under anoxic conditions. These findings collectively indicate that sequestering nitrogen in the ocean requires atmospheric oxidation to at least as oxidized as NO₂ and HNO₂.

We determine that the lifetime of molecular nitrogen is well longer than 1 billion years unless the NO flux is > 100 times larger than the present-day Earth's lightning production rate. As such, N₂ atmospheres on Archean Earth and habitable exoplanets of both Sun-like and M dwarf stars are kinetically stable against aqueous-phase sequestration. This result affirms the nitrogen-based habitability on rocky planets.

This research was supported by NASA's Exoplanets Research Program grant #80NM0018F0612. The research was carried out at the Jet Propulsion Laboratory, California Institute of Technology, under a contract with the National Aeronautics and Space Administration.

REFERENCES

- Broecker, W., & Peng, T. 1982, Lamont-Doherty Geological Observatory, Columbia University, Palisades, New York, 10964, 690
- Buchwald, C., Grabb, K., Hansel, C. M., & Wankel, S. D. 2016, *Geochimica et Cosmochimica Acta*, 186, 1
- Carpenter, L. J., & Nightingale, P. D. 2015, *Chemical reviews*, 115, 4015
- Des Marais, D., O Harwit, M., Jucks, K., et al. 2002, *Astrobiology*, 2, 153
- Domagal-Goldman, S. D., Segura, A., Claire, M. W., Robinson, T. D., & Meadows, V. S. 2014, *ApJ*, 792, 90
- France, K., Loyd, R. O. P., Youngblood, A., et al. 2016, *ApJ*, 820, 89
- Gao, P., Hu, R., Robinson, T. D., Li, C., & Yung, Y. L. 2015, *ApJ*, 806, 249
- Goldblatt, C., Claire, M. W., Lenton, T. M., et al. 2009, *Nature Geoscience*, 2, 891
- Grabb, K. C., Buchwald, C., Hansel, C. M., & Wankel, S. D. 2017, *Geochimica et Cosmochimica Acta*, 196, 388
- Gratzel, M., Taniguchi, S., & Henglein, A. 1970, *Ber Bunsenges Phys Chem*, 74, 1003
- Halevy, I., & Bachan, A. 2017, *Science*, 355, 1069
- Harman, C., Felton, R., Hu, R., et al. 2018, *ApJ*, 866, 56
- Harman, C. E., Schwieterman, E. W., Schottelkotte, J. C., & Kasting, J. F. 2015, *ApJ*, 812, 137
- Hu, R. 2013, PhD thesis, Massachusetts Institute of Technology
- Hu, R., Seager, S., & Bains, W. 2012, *ApJ*, 761, 166
- Hu, R., Seager, S., & Bains, W. 2013, *ApJ*, 769, 6
- James, T., & Hu, R. 2018, *ApJ*, 867, 17
- Jones, L. C., Peters, B., Lezama Pacheco, J. S., Casciotti, K. L., & Fendorf, S. 2015, *Environmental science & technology*, 49, 3444
- Kasting, J. F., & Walker, J. C. 1981, *Journal of Geophysical Research: Oceans*, 86, 1147
- Kasting, J. F., Whitmire, D. P., & Reynolds, R. T. 1993, *Icarus*, 101, 108
- Kharecha, P., Kasting, J., & Siefert, J. 2005, *Geobiology*, 3, 53
- Krissansen-Totton, J., Arney, G. N., & Catling, D. C. 2018, *Proceedings of the National Academy of Sciences*, 115, 4105
- Laneuville, M., Kameya, M., & Cleaves, H. J. 2018, *Astrobiology*, 18, 897
- Lee, Y.-N. 1984, Atmospheric aqueous-phase reactions of nitrogen species, Tech. rep., Brookhaven National Lab., Upton, NY (USA)
- Mancinelli, R. L., & McKay, C. P. 1988, *Origins of Life and Evolution of the Biosphere*, 18, 311
- Mather, T. A., Pyle, D. M., & Allen, A. G. 2004, *Geology*, 32, 905

- McKay, C. P., Scattergood, T. W., Pollack, J. B., Borucki, W. J., & Van Ghysseghem, H. T. 1988, *Nature*, 332, 520
- Miranda, K. M. 2005, *Coordination Chemistry Reviews*, 249, 433
- Navarro-González, R., Molina, M. J., & Molina, L. T. 1998, *Geophysical Research Letters*, 25, 3123
- Ranjan, S., Todd, Z. R., Rimmer, P. B., Sasselov, D. D., & Babbin, A. R. 2019, *Geochemistry, Geophysics, Geosystems*, 20, 2021
- Rugheimer, S., & Kaltenegger, L. 2018, *The Astrophysical Journal*, 854, 19
- Schumann, U., & Huntrieser, H. 2007, *Atmospheric Chemistry and Physics*, 7, 3823
- Seddon, W., Fletcher, J., & Sopchyshyn, F. 1973, *Canadian Journal of Chemistry*, 51, 1123
- Segura, A., Kasting, J. F., Meadows, V., et al. 2005, *Astrobiology*, 5, 706
- Shafirovich, V., & Lyman, S. V. 2002, *Proceedings of the National Academy of Sciences*, 99, 7340
- Stanton, C. L., Reinhard, C. T., Kasting, J. F., et al. 2018, *Geobiology*, 16, 597
- Summers, D. P., & Khare, B. 2007, *Astrobiology*, 7, 333
- Tian, F., France, K., Linsky, J. L., Mauas, P. J., & Vieytes, M. C. 2014, *Earth and Planetary Science Letters*, 385, 22
- Vladilo, G., Murante, G., Silva, L., et al. 2013, *The Astrophysical Journal*, 767, 65
- Walker, J. C., Hays, P., & Kasting, J. F. 1981, *Journal of Geophysical Research: Oceans*, 86, 9776
- Wong, M. L., Charnay, B. D., Gao, P., Yung, Y. L., & Russell, M. J. 2017, *Astrobiology*, 17, 975
- Wordsworth, R. D., & Pierrehumbert, R. T. 2013, *The Astrophysical Journal*, 778, 154
- Yung, Y., & McElroy, M. 1979, *Science*, 203, 1002
- Zafiriou, O. C. 1974, *Journal of Geophysical Research*, 79, 4491